Progress In Electromagnetics Research B, Vol. 51, 407–425, 2013

A PARETO ELITE SELECTION GENETIC ALGORITHM FOR RANDOM ANTENNA ARRAY BEAMFORMING WITH LOW SIDELOBE LEVEL

Suhanya Jayaprakasam*, Sharul K. A. Rahim, and Chee Y. Leow

Wireless Communication Centre (WCC), Faculty of Electrical Engineering, Universiti Teknologi Malaysia, UTM Skudai 81310, Malaysia

Abstract—Random antenna array (RAA) that uses the conventional beamforming method produces a poor beam pattern with high sidelobe level. This greatly reduces the performance and the efficiency of the antenna. The use of Genetic Algorithm (GA) to find the best positions for the antenna elements in RAA to lower the sidelobes has been widely researched. However, there has been no solution proposed for the reduction of sidelobes when the user has no autonomy over the position of the radiating elements, for instance in cases such as emergency communications. This paper proposes a novel Pareto Elite Selection Genetic Algorithm (PESGA) optimization method to reduce the sidelobes in an RAA that has fixed elements' position. The proposed method uses a single fitness function (peak sidelobe level) for parent selection while an additional function (number of sidelobes above a threshold level) is introduced to select the elitist in every generation via Pareto Front (PF) selection. Results indicate that the proposed PESGA method is best used for scenarios where the array size is small. In such cases, the proposed method provides much reduced sidelobe compared to the conventional RAA beamforming method and up to 200% improvements in terms of mainlobe to peak sidelobe ratio compared to GA weight optimized beamforming method.

Received 20 March 2013, Accepted 13 May 2013, Scheduled 15 May 2013

* Corresponding author: Suhanya Jayaprakasam (suhanya.jayaprakasam@gmail.com).

1. INTRODUCTION

Antenna array beamforming is a subset of smart antenna technology. It is used to improve the signal-to-noise and interference ratio (SINR) of a communication by directing the array's radiating power to specified bearings [1]. The recent roll-out of WiMAX and Long Term Evolution-Advanced (LTE-A) networks, which incorporates multiple input multiple output (MIMO) and beamforming capabilities has piqued the interest of communication scholars on antenna array beamforming techniques and performance analysis [2–6].

Initially, the research works on antenna array beamforming revolved around antenna arrays with elements set in uniform arrangements [1, 7]. The scope has now been extended to include arbitrarily placed antenna elements too, which form a random antenna array (RAA) [8–13]. An RAA consists of randomly placed antenna elements over a specified radius, which collectively forms an array for beamforming purposes. The applications of RAA can be broadly classified into two main classes: spatially perturbed RAA and spatially unperturbed RAA.

In spatially perturbed RAA, the arrangement of the antenna elements is deliberately computed and synthesized to be random. Though placed without a uniform arrangement, the position of each element is carefully calculated and chosen to achieve desired properties for the antenna radiation pattern. For example, the random element arrangement synthesis in [14] achieves accurate pointing and nulling in the beam pattern. The same author also presented an antenna pattern synthesis to attain broad nulling in [15]. The work in [16] meanwhile manipulated the spatial arrangement of the antenna to suppress the grating lobes in the beam pattern while [12] focused on achieving narrow beam and low side lobe level (SLL) in the radiation pattern.

On the other hand, spatially unperturbed RAA is a condition where the position of the elements in the array is random by nature, and it is not feasible to arrange elements of an array in a pre-computed fashion. The elements in the antenna array are fixed at random positions, and beamforming has to be achieved by using these randomly placed elements. An example of such application can be seen in the case of emergency communications as reported in [11]. Here, arbitrarily placed wireless transceivers act as an array that radiate a signal to emergency responders. Non-spatially perturbed RAA is also common in sensor networks [8]. Since the usually scattered sensor nodes' position cannot be changed, the array formed to beamform is random by nature and beamforming has to be achieved using these randomly placed elements. Seismic, ocean and air acoustic also applies

non-spatially perturbed RAAs [10].

Though the RAAs have its niche applications, it has to be noted that the SLLs of the RAAs also usually tend to be higher compared to uniform antenna arrays. One of the first articles describing the SLL problem in RAA was published in [17]. The author concluded that the number of elements influences the level of the largest SLL, or the peak sidelobe level (PSLL) to be higher compared to the PSLL of uniform arrays. Having high SLLs causes the antenna to incur interference with/to other radiating sources. This reduces the transmission and beam collection efficiency of the antenna.

Numerous approaches have been proposed to reduce the SLLs in antenna arrays. However, most works focus on SLL reduction for either arrays with uniform element arrangement [18–22], or on RAAs that fall into the first classification, namely the spatially perturbed RAA [10, 12, 14, 15, 20, 23, 24]. Literatures available on SLL reduction proposals for spatially unperturbed RAAs are fairly limited. An element selection method to reduce the SLLs for spatially unperturbed RAAs has been suggested in [25]. However, this scheme does not fully utilize all the available elements and power resources in the RAA, as some of the elements will be switched off during the beamforming process to achieve lower SLLs. Furthermore, the node selection method is only suitable to be used when the number of elements in the array is high.

A popular method in the literature to reduce the SLL in antenna arrays is by strategically placing the elements according to a set of pre-calculated optimum positions using optimization algorithms such as Genetic Algorithms (GA) [14, 20, 21], Particle Swarm Optimization [14, 20, 21, 26], Differential Evolution [27–31] and convex optimization [10, 12]. The position of the elements in the array is optimized via iterative procedures until the cost function of the algorithm, which is the PSLL, is minimized. This solution works well for spatially perturbed RAA. However, element positioning optimization is not a possible solution for the spatially unperturbed RAA, since the position of its elements cannot be manipulated.

The aforementioned optimization algorithms have also been used to optimize the weights that multiply the signals at each element, instead of optimizing the element position, to achieve a reduced SLL [18, 19, 22]. However, these approaches have only been adopted for arrays with uniform element arrangement. The works in [29–31] suggested a differential evolution optimization method to effectively beam towards angle of arrival and null out interferences in the presence of geometry estimation errors in uniform linear arrays. Nevertheless, the approach was not extended to achieve a lower overall SLL in the

radiation pattern.

In this paper, a solution to reduce the SLL for spatially unperturbed RAAs by optimizing the weight vector of the RAA is proposed. The proposed optimization technique, called Pareto Elite Selection Genetic Algorithm (PESGA), is a variant of the conventional GA.

Pareto optimal solution is an optimization approach that is used when multiple objectives exist in a problem. This approach ensures that the solution more or less equally satisfies all the objectives. In Pareto GA the objective functions are mapped against each other, and the non-dominated, optimal solutions form a Pareto Frontier (PF) in the objective function space [32–34]. The population is then ranked according to its dominance of the objective function map and consequently used for parent selection and crossover in GA.

Though the problem of reducing SLLs for spatially unperturbed RAAs is a single objective optimization, it is treated as a multi-objective optimization method in this paper by introducing a sub-objective in the existing GA. The sub-objective is to ensure that the number of SLLs above a fixed threshold is kept to a minimum. Unlike the existing Pareto GA that uses the Pareto mapping as the fitness function for parents selection purposes, the proposed PESGA selects the PF chromosomes as the elite that will be retained for its next generation.

The proposed method is applied to RAA set against 4 different scenarios, modeled to relate to practical applications. The array radiating power obtained using PESGA is compared to the radiating power of the original AF and the conventional GA. Further result analysis on PSL, gain and half power beamwidth (HPBW) is investigated out to prove the efficacy of the proposed solution.

2. MATHEMATICAL FORMULATION OF RANDOM ANTENNA ARRAY BEAMFORMING

The array factor (AF) for RAA is presented in this section. The AF presented here is simplified into a 2-dimensional (2D) AF from the original 3D representation in [35]. Consider a total of K elements in an RAA, with a geometrical composition as depicted in Figure 1, scattered within a radius of R meters. It is assumed that each element is equipped with a single isotropic antenna.

One of the elements in the array is engaged as the reference element, n_1. The element n_1 is referenced as the origin (0, 0) and is the geometrical reference point for all the other elements in the system. The radius position, r_k of the k-th element in the array, n_k is within

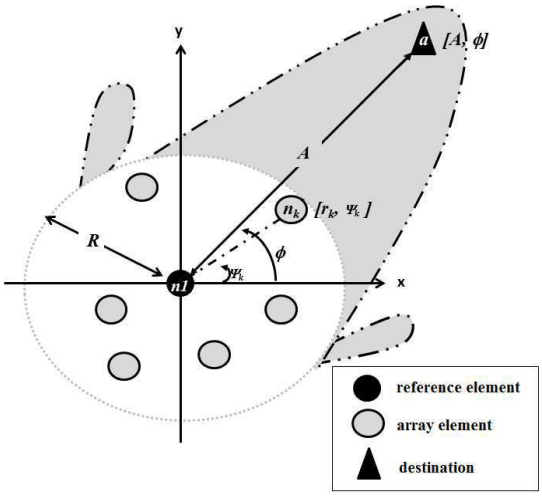

Figure 1. Geometrical configuration of collaborative beamforming.

the range of $0 \leq r_k \leq R$. Meanwhile, the elevation angle, Ψ_k of n_k is within the range of $-180^\circ \leq \Psi_k \leq 180^\circ$.

All the elements in the array is required to produce a beam towards a position, a, situated A meters with an elevation angle of ϕ relative to n_1. Far field position is assumed, hence $A \gg R$. The elevation angle ϕ can be assumed as the angle of arrival (AOA) for downlink transmit beamforming and as the signal of interest (SOI) for uplink receive beamforming. When far field condition is assumed, the resultant AF at $\theta \in [-180^\circ, 180^\circ]$ is:

$$AF(\theta, \sigma) = \frac{1}{K} \sum_{k=1}^{K} w_k \, e^{-j\frac{2\pi}{\lambda} r_k [\cos(\theta - \psi_k)]} \tag{1}$$

where w_k is the weight at the element k, represented by:

$$w_k = \sigma_k e^{j\frac{2\pi}{\lambda} r_k [\cos(\phi - \psi_k)]} \tag{2}$$

The energy, σ_k governs n_k's excitation amplitude, whereas $\cos(\phi - \psi_k)$ determines its excitation phase.

Each element multiplies the signal the corresponding weight to align the phase of the signal. This will ensure that signals from all the elements will be in-phase towards the direction a when radiated. Therefore the produced main beam will be directed towards a.

3. PARETO ELITE SELECTION GENETIC ALGORITHM FORMULATION

The procedure of implementing the proposed PESGA algorithm is explained in this section. With this method, dual objectives: the PSLL and the number of SLLs above a fixed threshold are treated as the cost functions.

The GA creates a population of solutions and applies genetic operators such as mutation and crossover to evolve the solutions in order to find the best solution. In the conventional RAA beamforming explained in the previous section, radiation pattern is produced with unity excitation amplitude. Both GA and PESGA is applied to obtain the optimum antenna elements excitation weight at each element of the RAA to shape the beam pattern with minimized SLL. The proposed PESGA in our system works to obtain the best weight for each element through series of populations as described here:

Step 1: Initial Population and Chromosome Construction. In a GA, a chromosome, c is a set of input variables consisting of K number of variables. The kth input variable corresponds to the excitation energy (amplitude) of weight at the kth antenna element, σ_k in the RAA. Each generation consists of P number of chromosomes, where P is the size of the population. Assuming that the GA is evaluated for a maximum of G generations, the chromosome population at the gth generation is represented as:

$$\mathbf{POP}\,(g) = [\mathbf{c_1} \ldots \mathbf{c_p} \ldots \mathbf{c_P}]^T \tag{3}$$

where $[\cdot]^T$ is a transpose operator and

$$\mathbf{c_p} = \left[\sigma_{(p,1)} \ldots \sigma_{(p,k)} \ldots \sigma_{(p,K)}\right]^T \tag{4}$$

with $p = [1, 2, \ldots, P]$ and $k = [1, 2, \ldots, K]$.

The initial power of each weight is set to be unity to represent a beamforming solution for RAA without optimization. Hence, the chromosome population during the initial generation, $\mathbf{POP}(1)$ is a unity matrix of P rows and K columns.

Step 2: Fitness Evaluation. Fitness function is formulated to evaluate the SLL power and get possible lowest PSLL power compared to the desired SLL power.

The angles of the local maxima (SLL peaks) for the AF are:

$$[\boldsymbol{\theta}_{\mathbf{SL}}] = \arg\max\left\{AF\,(\boldsymbol{\theta}, \mathbf{c_p})\right\} \tag{5}$$

where $\boldsymbol{\theta} \in [-180°,\ 180°]$; $\boldsymbol{\theta} \neq \phi$.

The first fitness function is the value of the PSLL:

$$f_1\,(\mathbf{c_p}) = \max\left\{20\log_{10} AF\,(\boldsymbol{\theta}_{\mathbf{SL}}, \mathbf{c_p})\right\} \tag{6}$$

A second fitness function is introduced to determine the number of SLL which is T dB lower than the PSLL.

$$f_2(\mathbf{c_p}) = |[20\log_{10} AF(\boldsymbol{\theta}_{\mathbf{SL}}, \mathbf{c_p}) > (f_1(\mathbf{c_p}) - T)]| \tag{7}$$

The term $|\cdot|$ represents the size of the vector.

Step 3: Parent Selection. Once initial population is generated, the parent selection process takes place. For this paper, ranking selection method was used. The ranking selection method chooses the chromosome with high fitness level from the parent and discards the lower fitness level. Hence, with a selection rate of X_{rate}, the top $X_{rate} * P$ of the chromosomes are chosen as the parents and the rest are discarded.

Step 4: Crossover and Mutation. A crossover point is randomly chosen and the part of chromosomes beyond and after the crossover points is swapped to form the offspring. After that, mutation process randomly changes some of the values in the genes into a random floating point within the range of 0 and 1, with a mutation rate of μ. These gene values correspond to the excitation energy (amplitude) of weight of the antenna elements. The recently mutated offspring population is evaluated based on the fitness function and ranked.

Step 5: Elite Selection. The fitness function f_1 and f_2 are mapped together. A chromosome has a Pareto optimal solution if no other chromosome dominates that solution with respect to the fitness functions. Chromosome $\mathbf{c}_1$ is said to dominate $\mathbf{c}_2$ if $\mathbf{c}_1$ has a lower cost than $\mathbf{c}_2$ for f_1, and is not worse with respect to f_2. This can be expressed as:

$$f_1(\mathbf{c}_1) < f_1(\mathbf{c}_2) \quad \text{and} \quad f_2(\mathbf{c}_1) \leq f_2(\mathbf{c}_2) \tag{8}$$

Once the set of Pareto optimal solutions is found, the chromosomes of this set are chosen as the elite for the next generation. These chromosomes are not subjected to the crossover and mutation process.

Step 6: Convergence Check. The algorithm is stopped when the maximum number of iteration, G is reached or when the cost function, $f_1(\mathbf{c_p})$ is smaller than the user defined threshold, $PSLL_{\min}$.

Step 7: Projection and re-iteration. The iteration index is updated to $g = g + 1$, and go to Step 2.

4. NUMERICAL RESULTS

Four scenarios are formulated to analyze the performance of the proposed PESGA weight selection algorithm for PSLL reduction in RAA. Each element is equipped with an omni-directional antenna. It is assumed that the controller has knowledge on the position of the

all nodes a priory. The scenarios and the practical examples which corroborates with each scenario are as follows:

Scenario 1: 5 elements ($N = 5$) are randomly distributed over a disk with radius $R = \lambda$, and SOI/AOA at $-35°$. This scenario depicts a case where low number of closely spaced elements is available to form a RAA for beamforming purpose, such as in emergency communications.

Scenario 2: 100 elements ($N = 100$) are randomly distributed over a disk with radius $R = \lambda$, and SOI/AOA at $0°$. A clear example of such scenario is the case of beamforming in wireless sensor networks (WSNs).

Scenario 3: 7 elements ($N = 7$) are randomly distributed over a disk with radius $R = 1000\lambda$, and SOI/AOA at $-10°$. This scenario gives a picture of a case where low numbers of sparsely and randomly spaced elements collaboratively beamform. An example of such scenario is collaborative beamforming between base stations in cellular communications.

Scenario 4: 100 elements ($N = 100$) are randomly distributed

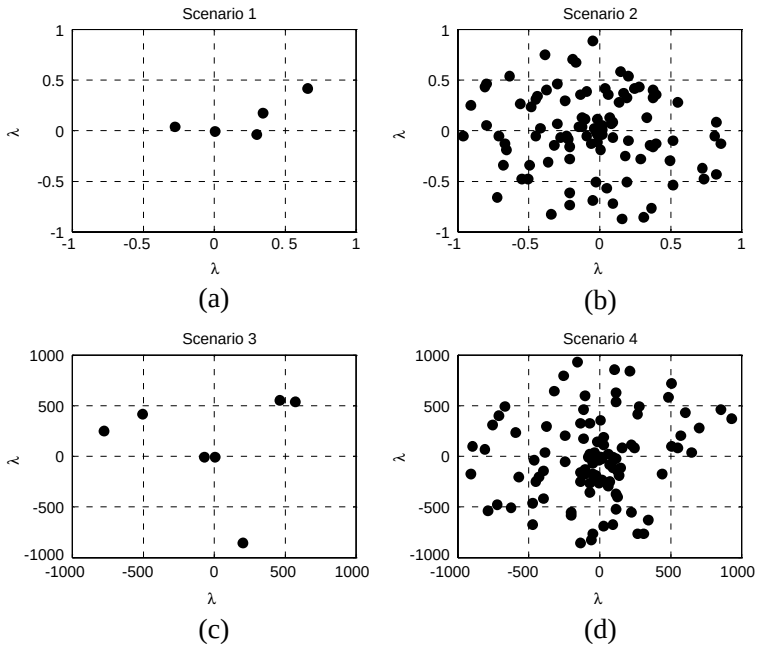

Figure 2. Arrangement of elements or the following scenarios. (a) $N = 5$, $R = \lambda$. (b) $N = 7$, $R = 1000\lambda$. (c) $N = 100$, $R = 1000\lambda$. (d) $N = 100$, $R = \lambda$.

over a disk with radius $R = 1000\lambda$, and SOI/AOA at 35°. This scenario depicts a case where high density of elements distributed in a large space forming an RAA to beamform. An example of such scenario is collaborative beamforming among nodes in a hotspot/Wi-Fi area to communicate with the access point (AP).

All random distributions follow a uniform distribution function. Sample of arrangement of elements for each scenario is illustrated in Figure 2. The four distributions shown in the figure represent N number of elements and disk size R that has been explained in Scenarios 1 to 4, accordingly.

To illustrate the PF elite selection method, the plot of objectives at the 2nd, 20th and 200th generation for Scenario 4 is shown in Figure 3. The lines that connect the points in the figure are the Pareto front of each generation. The chromosomes of the points which form the Pareto front in each generation is retained as the elitist in the next generation.

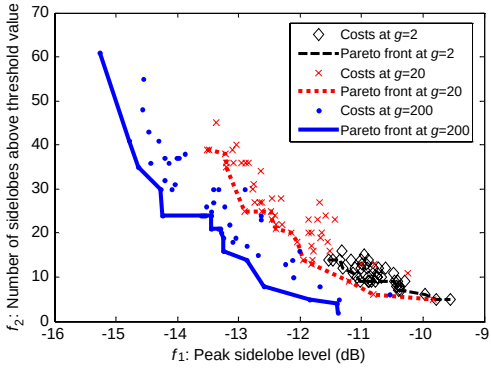

Figure 3. Plot of objectives and the corresponding Pareto front for Scenario 4 at the 2nd, 20th and 200th generation.

The parameters used for the GA weight optimization algorithm are $P = 100$, $G = 200$, $X_{rate} = 0.5$, $\mu = 0.01$. For the proposed T is set to 3 dB.

The proposed PESGA-RAA beamforming method is compared to the conventional RAA beamforming and GA-RAA beamforming. The resultant optimal excitation weights for the Scenario 1 and Scenario 3 are compared in Table 1 and Table 2, respectively. These weight values, along with the provided element position (r_k and ϕ_k), can be used to recreate the optimized beampattern using Equation (1). The weights of Scenario 2 and 4 are not shown due to the large number of elements. We can observe from the weights of RAA, GA-RAA and PESGA-RAA in the Tables 1 and 2 that not all elements undergo changes in its final

Table 1. Optimal weights values for Scenario 1.

k	r	ϕ	W_{RAA}	$W_{GA\text{-}RAA}$	$W_{PESGA\text{-}RAA}$
1	0	0°	$1.0000 + 0.0000i$	$1.0000 + 0.0000i$	$1.0000 + 0.0000i$
2	0.258λ	32.44°	$-0.2881 + 0.9576i$	$-0.2881 + 0.9576i$	$-0.2881 + 0.9576i$
3	0.130λ	26.58°	$0.3971 + 0.9178i$	$0.2668 + 0.6105i$	$0.1801 + 0.4095i$
4	0.099λ	-8.64°	$-0.1151 + 0.9934i$	$-0.1151 + 0.9934i$	$-0.1151 + 0.9934i$
5	0.092λ	173.0°	$0.0426 - 0.9991i$	$0.0426 - 0.9991i$	$0.0428 - 0.9965i$

Table 2. Optimal weights values for Scenario 3.

k	r	ϕ	W_{RAA}	$W_{GA\text{-}RAA}$	$W_{PESGA\text{-}RAA}$
1	0	0°	$1.0000 - 0.0000i$	$1.0000 - 0.0000i$	$0.8090 + 0.5878i$
2	272.4λ	162.6°	$0.5574 - 0.8303i$	$0.0322 - 0.0443i$	$0.0165 - 0.0199i$
3	217.5λ	140.7°	$0.7357 + 0.6773i$	$0.7357 + 0.6773i$	$0.7357 + 0.6773i$
4	23.6λ	-175.3°	$-0.9808 - 0.1953i$	$-0.9808 - 0.1953i$	$-0.0288 - 0.0074i$
5	239.0λ	49.92°	$-0.8565 - 0.5162i$	$-0.8565 - 0.5162i$	$-0.8565 - 0.5162i$
6	292.9λ	-76.9°	$0.8266 - 0.5628i$	$-0.0504 + 0.0375i$	$0.8266 - 0.5628i$
7	261.1λ	43.67°	$-0.9839 + 0.1786i$	$-0.0156 - 0.0281i$	$0.0611 - 0.0139i$

weight. For example only element 3 and 5 differs for the weights of Scenario 1. Similarly for Scenario 3 from Table 3, elements 3 and 5 retain the same weight as conventional RAA beamforming in both GA-RAA and PESGA-RAA. The weights of the elements not only determine the SLL, but also steers the main lobe level (MLL) towards the SOI/AOA. Since the SOI/AOA of the array is kept constant, certain level of similarity between the RAA, GA-RAA and PESGA-RAA weights is natural.

Meanwhile, the radiation patterns for Scenarios 1 to 4 are shown in Figure 4. From Figure 4(a), it is evident that PESGA could suppress the PSLL at the angle 140° better than the GA method and incurs minimal loss of gain at the MLL. The scenario for the radiation pattern Figure 4(b) differs from that of Figure 4(c) in terms of element density. The radiation pattern shows that PESGA successfully suppressed the PSLL by 24 dB. However, degradation in the MLL is also noticed for this case (-5 dB), though minimal when compared to the overall PSLL reduction.

The radiation pattern for a large disk RAA with low number of elements is shown in Figure 4(c). Result shows 2 dB of improvement in

Table 3. HPBW, MLL and MLL : PSLL improvement comparisons for Scenarios in Figure 2.

Scenario	**1st**	**2nd**	**3rd**	**4th**
Number of elements, N	**5**	**100**	**7**	**100**
Radius, R	λ	λ	1000λ	1000λ
AOA and SOI, ϕ	-35°	0°	-10°	35°
HPBW $\theta_{3\,\mathrm{dB}}$				
Initial	54.0°	39.0°	0.35°	0.25°
GA	58.0°	39.1°	0.68°	0.30°
PESGA	58.5°	42.5°	0.80°	0.32°
MLL **(dB)**				
Initial	0	0	0	0
GA	−0.0300	−3.3512	−0.5195	−0.6670
PESGA	−0.1922	−4.5513	−0.5413	−0.7513
MLL : PSLL **(dB)**				
Initial	5.8700	12.4650	0.9485	10.8485
GA	8.9530	28.8044	2.3513	13.9345
PESGA	9.8427	31.7022	2.6647	14.5760

the PSLL and −0.3 dB degradation in the MLL for PESGA compared to the conventional RAA beamforming. Figure 4(d) illustrate the result for an RAA of the same size but higher number of elements. The result records 5 dB improvement in the PSLL and around −0.7 dB in MLL degradation for PESGA when compared with the conventional RAA beamforming.

All the cases show that PESGA produces beampattern with lower PSLL over conventional GA and also beamforming without any optimization. Taking Scenario 1 in Figure 4(a) for example, the both GA and PESGA effectively produce radiation pattern lower than the initial PSLL of −5.87 dB. The result of PESGA manages to achieve PSLL lower than that produced by GA method by almost 1 dB, whereby GA achieves a −8.95 dB PSLL while PESGA achieves −9.84 dB.

A main point to note from Figures 4(a)–(d) is that elements which are positioned close to each other will produce radiation pattern with wide beamwidth, as can be seen in Figures 4(a) and (b) (Scenario 1 and 2, respectively). Wider beamwidth results in lower directivity of the antenna array, causing the system to be more susceptible to noise and interferences which are located close to SOI/AOA. However, the

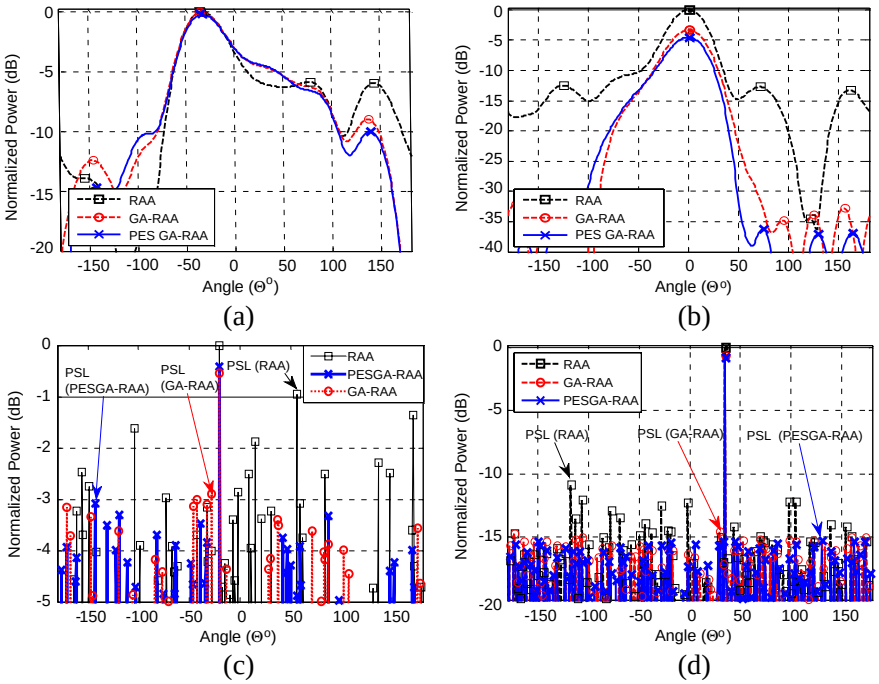

Figure 4. Radiation pattern for (a) Scenario 1, (b) Scenario 2, (c) Scenario 3, (d) Scenario 4.

wide beamwidth could be advantageous if the noise and interference level is low, since array with wider beamwidth is less affected by pointing errors. On the other hand, the total number elements in the array will affect the PSLL of the array, where higher number of elements would result in lower PSLL. This can be observed from the Figure 4(b) and Figure 4(d) ($N = 100$), which have much lower SLLs compared to Figure 4(a) and Figure 4(c) ($N = 5$ and 7, respectively).

The convergence graphs of the four methods are recorded to investigate the success of implementing conventional GA and PESGA on RAA beamforming (see Figure 5). From the graph, the convergence rate for PESGA is better than the GA for all cases and gives better PSLL towards the end.

However, both the GA and PESGA optimization methods cause reduction in the MLL's gain and increase of the half power beamwidth (HPBW) of the produced radiation pattern. The increase in HPBW is small enough to ignore, amounting to about 5° in Figure 4(a), for example. Meanwhile, the MLL's gain loss caused by the GA and

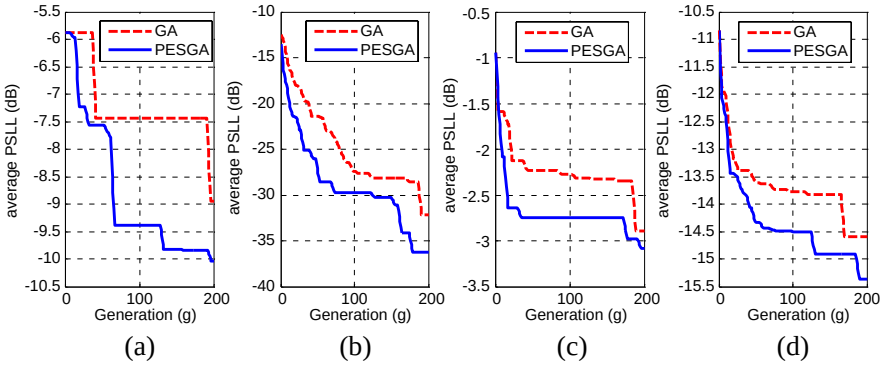

Figure 5. Comparative PSLL convergence graphs for GA and PESGA of scenarios in Figure 2. (a) Scenario 1. (b) Scenario 2. (c) Scenario 3. (d) Scenario 4.

PESGA method is compensated by the much lower PSLL produced by these methods, which ultimately provides better MLL to PSLL (MLL : PSLL) ratio.

Table 3 summarizes the properties for the normalized power (radiation patterns) for the 4 results illustrated in Figures 4(a)–(d), with elements arrangements shown in Figure 2. For all the cases, GA and PESGA are able to produce radiation pattern with suppressed PSLL, whereby PESGA solutions provide lower PSLL compared to GA solutions. The PESGA solution however suffers slightly higher MLL gain degradation compared to GA. Nevertheless, since the MLL : PSLL ratio of PESGA is higher compared to that of GA method, it can be concluded that the PESGA method can result in better SINR for the scenarios discussed. Better SINR improves the quality of the wireless communication as it ensures that the signal from SOI/AOA has much higher power compared to interferences and noise from other directions.

PESGA-RAA also records a slightly higher HPBW compared to the GA-RAA optimization method. However, the increase is very minimal and is less likely to cause any disadvantage to the overall system.

Due to the arbitrary crossover and mutation process in the GA, the weight distribution and the obtained optimized beam pattern may not be the same even if the process is repeated on the same arrangement of RAA. To acquire a better overall view and to validate the consistency on the improvement provided by the proposed algorithm, Monte Carlo approach for 100 different sets of array arrangement, repeated 10 times for each arrangement, for the 4 scenarios analyzed in this paper. The

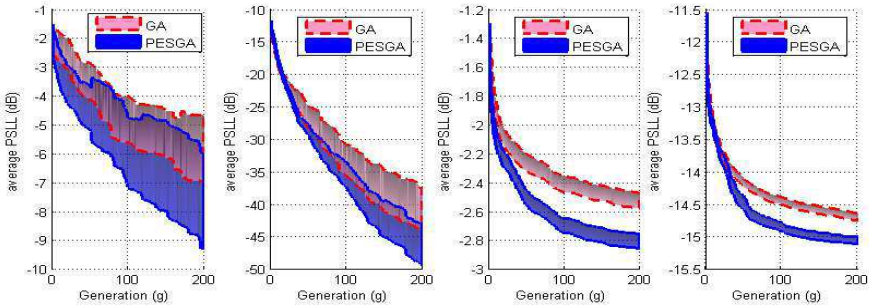

Figure 6. Average PSLL convergence graphs for GA and PESGA of scenarios 1 to 4, with 95% confidence limits. (a) Scenario 1. (b) Scenario 2. (c) Scenario 3. (d) Scenario 4.

Table 4. Average HPBW, MLL and MLL : PSLL improvement comparisons for the four scenarios.

Scenario	**1st**	**2nd**	**3rd**	**4th**
Number of elements, N	**5**	**100**	**7**	**100**
Radius, R	**λ**	**λ**	**1000λ**	**1000λ**
AOA and SOI, ϕ		**$-180° < \phi < 180°$**		
***HPBW*, $\theta_{3\,\mathrm{dB}}$**				
Initial	50°	37°	0.50°	0.27°
GA	52°	40°	0.54°	0.27°
PESGA	55°	40°	0.58°	0.28°
***MLL* (dB)**				
Initial	0	0	0	0
GA	−1.7457	−3.8683	−0.2583	−0.5355
PESGA	−2.0664	−3.0310	−0.2348	−0.4737
***MLL : PSLL* (dB)**				
Initial	2.2629	12.4075	1.3534	11.9437
GA	4.5175	39.0362	2.2816	14.2673
PESGA	6.9253	42.3821	2.5629	14.5861

results are recorded in Figure 6 and Table 4.

The convergence graph for the average PSLL improvements with 95% confidence limits is shown in Figure 6 and the average values for the MLL, HPBW and MLL : PSLL ratio are tabulated in Table 4. It is evident that the proposed PESGA-RAA method outperforms the

GA-RAA optimization method in all 4 scenarios in terms of PSLL. The increase in the HPBW for all cases is small enough to be ignored.

Both the GA and PESGA optimization methods cause degradation in the MLL to a certain extent. The effect of MLL degradation is more prominent when elements are positioned close to each other. This is however compensated by the improvement shown in the MLL : PSLL ratio. The average results shows that PESGA-RAA could provide better MLL : PSLL ratio for all the four scenarios compared to conventional RAA beamforming and GA-RAA.

Though PESGA method provide better result for all the scenarios, the MLL : PSLL improvement for the cases when the array size is large (Scenarios 3 and 4) is minimal compared to the GA method, amounting to less than 0.3 dB (∼107% improvement). On the other hand, when array size is small (Scenarios 1 and 2), we can obtain an improvement up to 3 dB (∼200%) in the MLL : PSLL ratio, compared to the GA method. This improvement in MLL : PSLL ratio ensures a better SINR and hence improves the quality of the communications system.

Since the proposed method is a form of evolutionary technique, it is expected to have high computational complexity. Therefore, more CPU time will be needed to execute the algorithm compared to the conventional beamforming method. An Intel(R) Core i7-3770 processor with 3.4 GHz speed and 32 GB RAM was used to run the simulations in this paper. The execution time for conventional RAA, GA and PESGA beamforming for Scenario 1 with 5 elements were measured around 0.084 seconds, 7.67 seconds and 7.73 seconds respectively. The execution time increases as the number of elements in the array increases due to the additional signal processing required. Therefore, the execution time for conventional RAA, GA and PESGA beamforming for Scenario 4 with 100 elements were comparatively higher, measuring around 0.730784 seconds, 131.492253 seconds and 131.502486 seconds respectively.

Both GA and PESGA record much higher computational time due to the iterative procedures involved in these two algorithms. The proposed PESGA's computational time is only slightly higher than the conventional GA method. For applications of the algorithm, a Graphic Processing Unit (GPU) or Field Programmable Gate Array (FPGA) can be used to make the algorithm execution much faster [30, 36, 37].

5. CONCLUSIONS

A procedure for reducing the level of the PSLL of RAAs made of random spacing arrays has been presented in this paper. A new algorithm-PESGA, which efficiently determines the optimum

excitation weight vector of the antenna element to produce beam pattern with lower SLLs has been proposed. Results for optimized random AFs having suppressed SLLs are compared with those of the conventional beam pattern and the conventional genetic algorithm optimization method. Four setting of RAA with varying element number and array size were analysed. In all cases, the proposed method suppresses the PSLL more effectively than the conventional GA method. Although the gain of MLL of PESGA-RAA is reduced compared to that of GA-RAA, the PESGA-RAA remains as the better solution as it yields better MLL to PSLL ratio, which assists in achieving better SINR in the communication system. Results show significant improvement in the MLL:PSLL for cases where the size of the RAA is small.

ACKNOWLEDGMENT

This work is supported in part by the Universiti Teknologi Malaysia's Research Grant under Project Vote No. Q.J130000.2523.02H92 and R.J130000.7723.4P029.

REFERENCES

1. John, L. and K. L. Titus, *Digital Beamforming in Wireless Communications,* Artech House, Inc., 1996.
2. Dahrouj, H. and Y. Wei, "Coordinated beamforming for the multicell multi-antenna wireless system," *IEEE Transactions on Wireless Communications*, Vol. 9, 1748–1759, 2010.
3. Muhammad, N., et al., "Beam forming networks using reduced size butler matrix," *Wireless Personal Communications*, 1–20, 2010.
4. Li, Q., et al., "MIMO techniques in WiMAX and LTE: A feature overview," *IEEE Communications Magazine*, Vol. 48, 86–92, 2010.
5. Shilo, S., A. J. Weiss, and A. Averbuch, "Performance of optimal beamforming with partial channel knowledge," *IEEE Transactions on Wireless Communications*, Vol. 10, 4035–4040, 2011.
6. Huang, Y., "WiMAX dynamnic beamforming antenna," *IEEE Aerospace and Electronic Systems Magazine*, Vol. 23, 26–31, 2008.
7. Constantine, A. B., *Antenna Theory: Analysis and Design*, Wiley-Interscience, 2005.
8. Huang, J. Y., P. Wang, and Q. Wan, "Collaborative beamforming for wireless sensor networks with arbitrary distributed sensors," *IEEE Communications Letters*, Vol. 16, 1118–1120, 2012.

9. D'Urso, M., M. G. Labate, A. Buonanno, and P. Vinetti, "Effective beam forming networks for large arbitrary array of antennas," *IEEE Transactions on Antennas and Propagation*, Vol. 60, 5129–5135, 2012.
10. Gerstoft, P. and W. S. Hodgkiss, "Improving beampatterns of two-dimensional random arrays using convex optimization," *Journal of the Acoustical Society of America*, Vol. 129, EL135–EL140, 2011.
11. Young, W. F., E. F. Kuester, and C. L. Holloway, "Measurements of randomly placed wireless transmitters used as an array for receivers located within the array volume with application to emergency responders," *IEEE Transactions on Antennas and Propagation*, Vol. 57, 241–247, 2009.
12. Fuchs, B. and J. J. Fuchs, "Optimal narrow beam low sidelobe synthesis for arbitrary arrays," *IEEE Transactions on Antennas and Propagation*, Vol. 58, 2130–2135, 2010.
13. Krishnamurthy, S., D. W. Bliss, and V. Tarokh, "Sidelobe level distribution computation for antenna arrays with arbitrary element distributions," *2011 Conference Record of the Forty Fifth Asilomar Conference on Signals, Systems and Computers (ASILOMAR)*, 2045–2050, 2011.
14. Li, W. T., X. W. Shi, L. Xu, and Y. Q. Hei, "Improved GA and PSO culled hybrid algorithm for antenna array pattern synthesis," *Progress In Electromagnetics Research*, Vol. 80, 461–476, 2008.
15. Li, R., L. Xu, X. W. Shi, N. Zhang, and Z. Q. Lv, "Improved differential evolution strategy for antenna array pattern synthesis problems," *Progress In Electromagnetics Research*, Vol. 113, 429–441, 2011.
16. Lu, B., S. X. Gong, S. A. Zhang, Y. Guan, and J. Ling, "Optimum spatial arrangement of array elements for suppression of grating-lobes of radar cross section," *IEEE Antennas and Wireless Propagation Letters*, Vol. 9, 114–117, 2010.
17. Steinberg, B., "The peak sidelobe of the phased array having randomly located elements," *IEEE Transactions on Antennas and Propagation*, Vol. 20, 129–136, 1972.
18. Zaharis, Z. D., K. A. Gotsis, and J. N. Sahalos, "Adaptive beamforming with low side lobe level using neural networks trained by mutated boolean PSO," *Progress In Electromagnetics Research*, Vol. 127, 139–154, 2012.
19. Zaharis, Z. D., C. Skeberis, and T. D. Xenos, "Improved antenna array adaptive beamforming with low side lobe level using a novel adaptive invasive weed optimization method," *Progress In Electromagnetics Research*, Vol. 124, 137–150, 2012.

20. Son, S. H. and U. H. Park, "Sidelobe reduction of low-profile array antenna using a genetic algorithm," *ETRI Journal*, Vol. 29, 95–98, 2007.
21. Lin, Z. Q., M. L. Yao, and X. W. Shen, "Sidelobe reduction of the low profile multi-subarray antenna by genetic algorithm," *AEU — International Journal of Electronics and Communications*, Vol. 66, 133–139, 2012.
22. Rocca, P., R. L. Haupt, and A. Massa, "Sidelobe reduction through element phase control in uniform subarrayed array antennas," *IEEE Antennas and Wireless Propagation Letters*, Vol. 8, 437–440, 2009.
23. Li, X., W.-T. Li, X.-W. Shi, J. Yang, and J.-F. Yu, "Modified differential evolution algorithm for pattern synthesis of antenna arrays," *Progress In Electromagnetics Research*, Vol. 137, 371–388, 2013.
24. Bevelacqua, P. J. and C. A. Balanis, "Optimizing antenna array geometry for interference suppression," *IEEE Transactions on Antennas and Propagation*, Vol. 55, 637–641, 2007.
25. Ahmed, M. F. A. and S. A. Vorobyov, "Sidelobe control in collaborative beamforming via node selection," *IEEE Transactions on Signal Processing*, Vol. 58, 6168–6180, 2010.
26. Liu, D., Q. Feng, and W.-B. Wang, "Discrete optimization problems of linear array synthesis by using real number particle swarm optimization," *Progress In Electromagnetics Research*, Vol. 133, 407–424, 2013.
27. Li, R., L. Xu, X.-W. Shi, N. Zhang, and Z.-Q. Lv, "Improved differential evolution strategy for antenna array pattern synthesis problems," *Progress In Electromagnetics Research*, Vol. 113, 429–441, 2011.
28. Mandal, A., H. Zafar, S. Das, and A. V. Vasilakos, "Efficient circular array synthesis with a memetic differential evolution algorithm," *Progress In Electromagnetics Research B*, Vol. 38, 367–385, 2012.
29. Mallipeddi, R., J. P. Lie, P. N. Suganthan, S. G. Razul, and C. M. S. See, "A differential evolution approach for robust adaptive beamforming based on joint estimation of look direction and array geometry," *Progress In Electromagnetics Research*, Vol. 119, 381–394, 2011.
30. Mallipeddi, R., J. P. Lie, P. N. Suganthan, S. G. Razul, and C. M. S. See, "Near optimal robust adaptive beamforming approach based on evolutionary algorithm," *Progress In Electromagnetics Research B*, Vol. 29, 157–174, 2011.

31. Mallipeddi, R., J. P. Lie, P. N. Suganthan, S. G. Razul, and C. M. S. See, "Robust adaptive beamforming based on covariance matrix reconstruction for look direction mismatch," *Progress In Electromagnetics Research Letters*, Vol. 25, 37–46, 2011.
32. Zitzler, E. and L. Thiele, "Multiobjective evolutionary algorithms: A comparative case study and the strength Pareto approach," *IEEE Trans. Evol. Comput.*, 257–271, 1999.
33. Haupt, R. L. and S. E. Haupt, *Practical Genetic Algorithms*, 2nd Edition, John Wiley & Sons Inc., Hoboken, New Jersey, 2004.
34. Goudos, S. K., K. Siakavara, E. Vafiadis, and J. N. Sahalos, "Pareto optimal Yagi-Uda antenna design using multi-objective differential evolution," *Progress In Electromagnetics Research*, Vol. 105, 231–251, 2010.
35. Ochiai, H., P. Mitran, H. V. Poor, and V. Tarokh, "Collaborative beamforming for distributed wireless ad HOC sensor networks," *IEEE Transactions on Signal Processing*, Vol. 53, 4110–4124, 2005.
36. Dikmese, S., A. Kavak, K. Kucuk, S. Sahin, and A. Tangel, "FPGA based implementation and comparison of beamformers for CDMA2000," *Wirel. Pers. Commun.*, Vol. 57, 233–253, 2011.
37. Zaharis, Z. D. and T. V. Yioultsis, "A novel adaptive beamforming technique applied on linear antenna arrays using adaptive mutated boolean PSO," *Progress In Electromagnetics Research*, Vol. 117, 165–179, 2011.